frontiers in Remote Sensing

TYPE Original Research
PUBLISHED 05 June 2026
DOI 10.3389/frsen.2026.1703257

OPEN ACCESS

EDITED BY
Juan Jose Munoz-Perez,
University of Cádiz, Spain

REVIEWED BY
Ana Laura Delgado,
CONICET Instituto Argentino de Oceanografía (IADO), Argentina
Asmita Singh,
Norwegian University of Science and Technology, Norway

*CORRESPONDENCE
Gavin H. Tilstone,
ghti@pml.ac.uk

RECEIVED 11 September 2025
REVISED 02 April 2026
ACCEPTED 27 April 2026
PUBLISHED 05 June 2026

CITATION
Tilstone GH and Land PE (2026) Decline in satellite-derived primary production in the north-east Atlantic driven by changes in sea surface temperature and mixed layer depth.
Front. Remote Sens. 7:1703257.
doi: 10.3389/frsen.2026.1703257

Decline in satellite-derived primary production in the north-east Atlantic driven by changes in sea surface temperature and mixed layer depth

Gavin H. Tilstone* and Peter E. Land

Plymouth Marine Laboratory, Plymouth, United Kingdom

Phytoplankton Primary Production supports most of the marine ecosystem and is highly sensitive to changing environmental pressures. There is much debate about whether marine primary production is increasing or decreasing and what environmental parameters may be driving these changes. We analysed a 21-year time-series of net primary production (NPP) computed from Ocean Colour Climate Change Initiative (OC-CCI) data spanning September 1997-December 2018, focusing on areas of similar phenology, climatology, and annual NPP in the north-east Atlantic Ocean. Across the entire area, NPP increased from 1998 to 2003, followed by a significant decline until 2018. This pattern was predominant in north-western European coastal waters and specific areas of the English Channel, Irish Sea, North Sea and Norwegian Sea, where it was related to changes in sea surface temperature and mixed layer depth.

KEYWORDS
anomalies, north atlantic ocean, phenology, phytoplankton, primary production, time series

1 Introduction

Primary production is fundamental for all life in the ocean, as it forms the base of the marine food web (Falkowski et al., 2004). Global marine net primary production (NPP) is almost equal to that of terrestrial ecosystems, and is estimated at 50 Pg C yr^{-1} (Field et al., 1998; Zhao and Running, 2010). Marine NPP has been reported to have increased over the past few decades (Chavez et al., 2011), yet other studies suggest a global decrease in phytoplankton biomass (Boyce et al., 2010). Contrasting patterns in NPP have been reported over the global ocean using different NPP models (Ryan-Keogh et al.,. 2023). Using ocean-colour satellite data from 1998 to 2015 to compute NPP, a small but significant decline of −0.8 PgC y^{-1} (−2.1%) $decade^{-1}$ has been recorded globally, which implies that the biological pump is weakening (Gregg and Rousseaux, 2019). A recent global analysis, using 25 years of satellite data, suggest that there is a significant decline in NPP in 50% of the global ocean, especially in tropical and subtropical stratified regions, which is driven by nutrient limitation (Silsbe et al., 2025).

In the North Atlantic and North Sea, contrasting trends in NPP have also been reported. At the Bermuda Atlantic Time Series (BATS) station, for example, Lomas et al. (2010) showed that NPP increased by approximately 60% during the winter to spring period between 1988 and 2007. In the adjacent subtropical North Atlantic Ocean an increase in productivity was also reported (Bates, 2017) due to more frequent and stronger storms leading to higher

water column mixing during winter and spring (Lomas et al., 2013). This may also be due to mesoscale eddies in the Sargasso Sea, which can elevate the annual nitrate supply (McGillicuddy et al., 1998). By contrast, Boyce et al. (2010) reported a decrease in NPP due to a decrease in nutrients and grazing. In the Iceland and Irminger basins, analysis of the satellite ocean colour record from 1997 to 2010, using two different models, showed a consistent decrease in NPP (Henson et al., 2010; Tilstone et al., 2015). Similarly in the North Sea, Capuzzo et al. (2018) used *in situ* measurements of chlorophyll-a (Chl *a*) and the underwater light field to compute NPP and found that there was a significant decline in NPP from 1988 to 2013, though the variability in photosynthetic rates was not included in the model. More recently, at the BATS station, *in situ* NPP exhibited a significant decline from 1997 to 2016 by 2.2 mg C m^2 d^{-1} per year with the largest decline of 9.3 mg C m^2 d^{-1} per year over the period from 2008 to 2016 (Wu et al., 2024). Similarly D'Alelio et al. (2020) reported a significant decrease in *in situ* NPP at BATS of 5.6 mg C m^2 d^{-1} per year from 1990 to 2016, which is related to a decline in total microplankton and a slow increase in the contribution of prokaryotes to NPP (Lomas et al., 2022). In the sub-tropical Atlantic at the CARIACO time-series station in the Caribbean, a similar significant decrease in *in situ* NPP of 8.5 mg C m^2 d^{-1} per year has been recorded from 1997 to 2016 (Wu et al., 2024) due to weakening of upwelling after 2003 in response to weakened trade winds and warming of the Atlantic. There has also been significant warming in the Azores region of the Atlantic of 2.7 °C per century, which has caused a decrease in NPP in the Canary upwelling system and expansion of open ocean areas of 10% from 1997 to 2019 (Siemer et al., 2021).

There is much interest in trends in NPP in the shadow of the global increase in sea surface temperature (SST) (Chavez et al., 2011). There can be variable and contrasting responses in phytoplankton photosynthetic rates to an increase in temperature, which can also increase photosynthetic rates to specific asymptotic limits (e.g., Xie et al., 2015), and therefore NPP, due to an increase in the Calvin cycle enzyme turnover (Raven et al., 2012). By contrast, increases in seawater temperature can also decrease NPP due to more persistent and deeper water column stratification that causes nutrient limitation (Beardall et al., 2009) and size- or taxon-specific changes to phytoplankton that have lower photosynthetic rates (Robinson et al., 2018).

The objective of this study is to assess changes in NPP in the north-east Atlantic and evaluate the environmental factors driving these changes, using over two decades of satellite data. The research is the companion study to Tilstone et al. (2023), which defined threshold indicators for primary production in the same regions and used them to assess environmental disturbances. The present study provides valuable insight into changes in NPP over a 21-year period and their relationship with environmental stressors.

2 Materials and methods

2.1 Remote sensing data

The study was conducted in the north-east Atlantic from 48° to 60°N, 15°W to 10°E (Figures 2, 3), which includes seasonally stratified, intermittently stratified and permanently mixed waters (van Leeuwen et al., 2015). We used daily OC-CCI (v4.2) Chl *a* data at 4 km resolution (https://climate.esa.int/en/projects/ocean-colour/data/) linearly interpolated to 0.05° resolution to calculate NPP from September 1997 to December 2018. Melin et al. (2017) showed that the trends in Chl *a* calculated with OC-CCI v4.2 time series are consistent with those calculated from single sensor products (SeaWiFS, MERIS, MODIS-Aqua, VIIRS), demonstrating the fitness of the data for time-series studies. In the processing versions of the OC-CCI products, v1 to 4 used SeaWiFS as the reference sensor, whereas v5 and 6 used MERIS to expand the overlap with other ocean colour sensors. Jackson et al. (2021) using 23 years of OC-CCI data showed that both v4 and v5 had the same trend in global Chl *a* with a decrease from 1999 to 2005, followed by an increase to 2011 and a steeper decrease to 2016. OC-CCI v5 did exhibit slightly higher median Chl *a* compared to v4.2. In addition, Kulk et al. (2020) used OC-CCI v4.1 to compute NPP both globally and at the basin scale and compared the trend in these data to those from *in situ* photosynthetic parameters and found the same trend. The OC-CCI Chl *a* is computed from the OC5CI algorithm using Remote Sensing Reflectance (R_{rs}), merged between SeaWiFS, MODIS-Aqua, MERIS, VIIRS and Sentinel-3 (Sathyendranath et al., 2019). OC5CI is a switching algorithm that applies the colour index (CI) in open-ocean, Case 1 waters and the OC5 model in coastal, Case 2 regions. OC5 is based on OC4 (O'Reilly et al., 2000), but accounts for the absorption of coloured dissolved organic matter (CDOM) and scattering of suspended particulate material (SPM), using an empirical parameterisation of the maximum normalised water leaving radiance band ratio at 412 and 560 nm, from a look-up-table (Novoa et al., 2012; Saulquin et al., 2011; Gohin et al., 2002). As a quality control measure, in coastal regions the method of Lavigne et al. (2021) was deployed to flag and mask pixels where the OC5CI algorithm is likely to fail. The Lavigne et al. (2021) Chl *a* algorithms utilise a combination of OC4, OC5 and NIR-RED algorithms applied on an optical water type basis. From the salient optical water types, the optical conditions (high, medium, low SPM, and CDOM) with which the OC4 and OC5 algorithms can provide reliable Chl *a* estimates, were chosen following Lee and Hu (2006). The NIR-RED algorithm of Ruddick et al. (2001), was selected for turbid waters with low Chl *a* concentrations based on both the Chl *a* concentration and reflectance in the near infra-red (NIR) bands. For the NIR-RED algorithm, the band usually used is 665 nm, but because the 665 nm band is affected by Chl *a* absorption, water reflectance at 620 nm was used as an index for water reflectance in the red.

2.2 Net primary production

The wavelength resolving NPP model of Morel (1991), as implemented by Smyth et al. (2005) was used. This model parameterises the maximum quantum yield for growth (ϕm) and the maximum phytoplankton Chl *a* - specific absorption coefficient (a^*max) from Chl *a* following Morel et al. (1996). The above-water spectral light field was generated using the Gregg and Carder (1990) model run at 5 nm wavelength and 30 min time resolution so that NPP can be integrated over the day. Meteorological and ozone data to drive the model were obtained from National Centers for Environmental Prediction (NCEP) and Earth-Probe Total Ozone

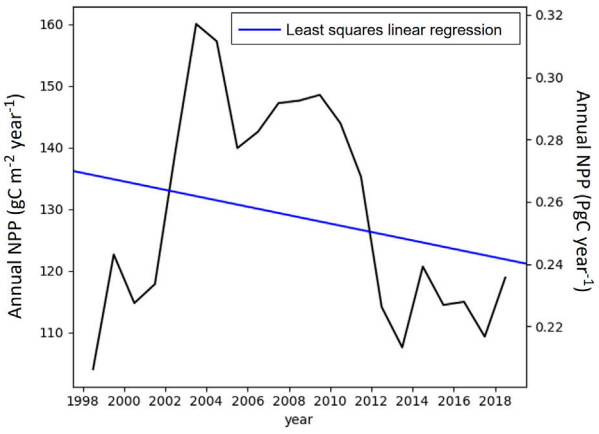

FIGURE 1
March to October net primary production (gC m^{-2} yr^{-1} on the left axis, regionally integrated in Pg C yr^{-1} on the right) using OC-CCI data for the north-east Atlantic. The blue line is a least squares linear regression through the gC m^{-2} yr^{-1} and PGC yr^{-1} data, showing an overall decline.

Mapping Spectrometer data (EPTOMS), respectively. Cloud fields were obtained from European Centre for Medium Range Weather Forecasts (ECMWF) model output and used to modify the above water light field following Reed (1977). The light field was propagated through the water column by calculating the spectral attenuation coefficient for downwelling irradiance following the methods of Morel (1988) as outlined in Tilstone et al. (2005). Hourly rates of NPP were weighted to the water column light field and carbon fixation was integrated over the light hours for each day down to 1% irradiance depth. Integration was performed over all daylight hours, for wavelengths 400–700 nm and computed through the iterative approach of Morel and Berthon (1989). The model was run using surface Chl *a* and temperature assuming a homogenous water column profile of Chl *a*, a*max and ϕm, since this is what is available from satellite. Phytoplankton Useable Radiation (PUR) irradiance was estimated using Morel (1991) and Photosynthetically Active Radiation (PAR) was derived from the Gregg and Carder (1990) model. To generate the time series of NPP, daily OC-CCI Chl *a*, SeaWiFS and MODIS PAR and the CMEMS global SST product (https://resources.marine.copernicus.eu/?option=com_csw&view=details&product_id=SST_GLO_SST_L4_REP_OBSERVATIONS_010_011) were used to compute daily and mean monthly satellite maps of NPP from September 1997 to December 2018. Mean annual maps of NPP from 1998 to 2018 were also generated to compute annual time-series trends (Figure 1). In addition, a daily map of the climatological mean NPP from 1997 to 2005 was also produced. Over the past 2 decades NASA have conducted five inter-comparisons of satellite models of NPP, to determine the most accurate models and to characterise sources of error (Campbell et al., 2002; Carr et al., 2006; Friedrichs et al., 2009; Saba et al., 2010; Saba et al., 2011; Lee, 2015). The Morel (1991) model as implemented by Smyth et al. (2005), ranked in the top four of the most accurate algorithms. In addition, continuous and extensive validation of the NPP model has been undertaken in the North Atlantic over the same study region over the past 16 years and multiple ocean colour missions (Tilstone et al., 2005; Robinson et al., 2009; Tilstone et al., 2009; Tilstone et al., 2015; Ford et al., 2021). These studies show that when the NPP model is applied to SeaWiFS and MODIS-Aqua the differences over these regions are between 15% and 35%.

2.3 Statistical methods

K-means clustering based on peak and timing of satellite NPP was used to identify regions with similar phenology and climatology using the methods detailed in Tilstone et al. (2023). Clustering used the following normalised climatological parameters: maximum NPP; the day number at which it occurs; annual NPP; latitude and longitude. Parameters are normalised by subtracting their NPP-weighted mean over the whole domain and dividing by the NPP-weighted standard deviation. Day number is normalised by calculating cos (2π dayNo/365) and sin (2π dayNo/365), as X and Y on an annual unit circle, finding the NPP-weighted mean of each and solving for the 'mean' dayNo. Adjusted dayNo is then dayNo-mean dayNo, adding 365 to values < -182.5, and this is normalised by dividing by its NPP-weighted standard deviation. It is possible to apply a similar logic to latitude and longitude, transforming them to X, Y and Z on a unit sphere, but since the domain is small, not elongated and far from the poles or the international dateline, latitude and longitude were normalised independently. The clustering is based on N = 11 regions (Tilstone et al., 2023; Figure 2). The optimum number of regions was checked using C indices (Hubert and Levin, 1976) and 9 and 11 regions were found to be optimum. The nine-region classification was rejected on the grounds that it did not distinguish the Irish and Celtic seas from the North Atlantic.

We assessed both the regional mean percentage trend in NPP over two periods, 1997–2005 and 2006–2018, and the correlation between monthly mean regional NPP and environmental variables that may affect NPP. The temporal split in the data was chosen for consistency and comparability with the companion study (Tilstone et al., 2023) and from trends reported in previous papers (e.g., Behrenfeld et al., 2006). Environmental variables investigated were the Atlantic Meridional Overturning Circulation index (AMOC; CMEMS Global Ocean Ensemble Physics Reanalysis. E.U, 2022), the El Niño Southern Oscillation index (ENSO; Wolter and Timlin, 2011), the North Atlantic Oscillation index (NAO; Barnston Livezey, 1987), and regional means of climatological mixed layer depth (MLD; CMEMS Global Ocean Ensemble Physics Reanalysis. E.U, 2022), SST, meridional and zonal winds (Hersbach et al., 2023). Climate indices and MLD were available as monthly averages, thus all other datasets, including NPP, were converted to monthly averages for comparison. All trends and correlations were calculated by least-squares linear regression of regional mean values. Regional trends in NPP can be strongly affected by trends in data gaps such as cloud cover. For instance, if cloud cover decreases in a highly productive subregion or season and increases in an unproductive subregion or season, a spurious increase in regional annual NPP will be observed. We ameliorated this in different ways for trends in daily NPP and for comparison with environmental variables. To assess trends in daily NPP, we subtracted daily climatological (1997–2005) pixel mean log (NPP) from daily log (NPP) to form a time series of the anomaly in log (NPP) from climatology, increasing the robustness of

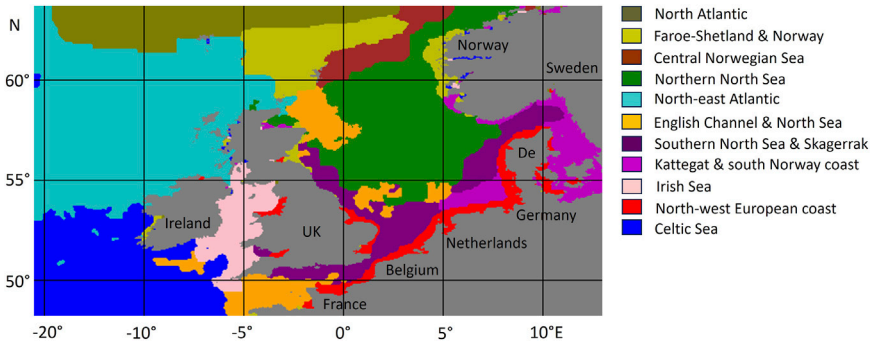

FIGURE 2
Regions of similar peak, timing, location and annual primary production identified using k-means cluster analysis. De is Denmark. Adapted from Figure 1 in Tilstone et al. (2023).

the time series to spatial NPP differences across the region and to the climatological seasonal cycle. The use of log (NPP) anomaly means that trends can be compared more easily, between high-NPP and low-NPP areas, and linear trends in log (NPP) anomaly can be converted into approximate percentage trends in NPP.

To assess the correlation between monthly NPP and environmental variables, linear use of NPP was more appropriate, and therefore the annual mean ratio of NPP to the climatology over each region was computed. Gaps in daily data due to clouds were replaced with the pixel climatology multiplied by that year's mean ratio. We then summed the gap-filled values alongside the actual values to produce a yearly mean NPP for each region. This means that the replacement data have the same annual percentage difference from climatology as the observed data in the same region. To avoid uninteresting correlations due to seasonality (e.g., both NPP and SST increase in summer, producing a strong correlation between NPP and SST that we have no interest in quantifying here), we calculated a running 12-month mean of each variable from the monthly means starting at each month of the time series, giving a total of 244 points for comparison. Note that this procedure means that each point shares data with its neighbours (e.g., Jan-Dec shares 11 of its 12 points with Feb-Jan), creating a local correlation between points even if none exists in the data. In contrast to the point cloud expected with uncorrelated data, this results in 'spaghetti' lines of points in the plots. This local inter-point correlation does not extend beyond 11 months and so should have minimal effect on the overall 21-year relationship between variables. Chl *a* and PAR were not included in the analysis, since these parameters are used to compute NPP directly and will inevitably result in a high correlation with NPP. Although SST is also used to compute NPP, its effect is much smaller than those of Chl *a* and PAR.

3 Results

Across the entire north-east Atlantic study area, mean March-October NPP increased between 1998 and 2003, then declined until 2013 after which it remained relatively constant (Figure 1). During the winter months, NPP is lower, and satellite estimates become less reliable, therefore these months were omitted from the analysis. The patterns of NPP trends varied between the 11 k-means regions. Maps of the relative trend in NPP (i.e., the annual increase or decrease in NPP expressed as a percentage) in each k-means region (Figure 2) over the growing season (March to October) from 1998 to 2005 and 2006 to 2018 are shown in Figure 3. Comparison of these sub-figures indicates that for regions west of 0° and the Kattegat and southern North Sea region around 55°N, 10°E, the NPP trend was significantly lower in 2006–2018 (Figure 3; Table 1).

Analysis of the trends in each month for the north-east Atlantic illustrated that during 1997–2005, an increasing trend in June-September weakened and shifted to September-October in 2006–2018. In addition, an increasing trend in March-April 1997–2005 weakened in 2006–2018, and there was generally a decreasing trend in other months and regions between these two periods (Figure 4). Of the 11 k-means areas (Figure 2), the decline in annual NPP over the whole time series from 1997 to 2018 was significant ($p<5\%$, two-tailed t-test) in all regions except the southern North Sea and the north-east Atlantic (Table 1).

To understand changes in the seasonal patterns, least-squares multilinear regression was used to relate NPP to environmental variables AMOC, ENSO, NAO, MLD, SST, meridional and zonal winds using 244 data points from the 21-year time series for each region. MLD, SST and winds were interpolated to 0.05° then averaged over each region. The strongest (highest r^2) correlations with other environmental parameters were in the Kattegat, northern North Sea, north-west European coast and the Irish Sea, where NPP decreased from 1997 to 2018 (Table 2; Figure 5). For the Kattegat (Figure 5a), the northern North Sea (Figure 5b) and the Irish Sea (Figure 5d), there was a slight decrease in annual NPP. The largest decline over the time series was in the north-west European coast (Table 1; Figure 5c). In the Kattegat and northern North Sea, SST and MLD explained 45% and 25% of the variability in mean annual NPP, respectively (Table 2). In the north-west European coastal region, 25% of the variability in mean annual NPP was explained by MLD and the NAO. Since NAO is derived from temperature differences, to compare with the other correlations, SST is plotted instead of NAO for the north-west European coast. In the Irish Sea, 21% of the variability in mean annual NPP was explained by SST and meridional winds (mwind; Table 2).

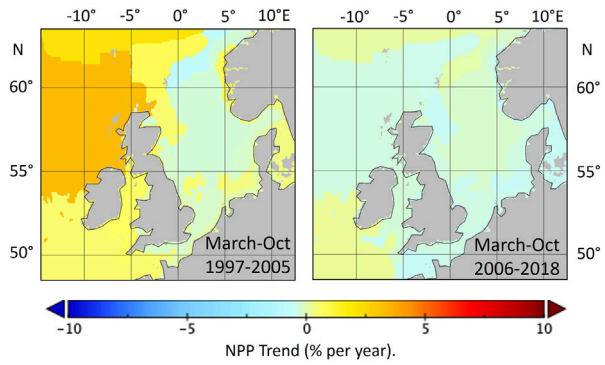

FIGURE 3
Regional significant trend in NPP (March-October) from 1997 to 2005 and 2006–2018 for k-means regions in the north-east Atlantic. Warm colours indicate an increase and cold colours indicate a decrease in NPP.

4 Discussion

4.1 Areas with similar primary production phenology, climatology and annual rates

For the north-east Atlantic, a k-means cluster analysis of monthly NPP had already identified 11 distinctive regions (Tilstone et al., 2023; Figure 2). These regions are similar to the new areas adopted by the Oslo Paris Convention (OSPAR) for the assessment of pelagic habitat and phytoplankton (Blauw et al., 2019; Devlin et al., 2023), derived from Sentinel-3 OLCI OC5 Chl *a* (Lavigne et al., 2021). The Irish Sea, English Channel, Northern North Sea and Kattegat were identified in both NPP and OC5 Chl *a* studies. The differences occurred in the Atlantic area, in which Tilstone et al. (2023) defined three areas of the Atlantic as North Atlantic, North-East Atlantic and Celtic Sea and the OC5 Chl *a* method had one large area. In addition, the Intermittently stratified and Eastern North Sea regions defined by Blauw et al. (2019), were classified as southern North Sea and Skagerrak by Tilstone et al. (2023). The North-West European coast and English Channel and North Sea defined in the NPP study were not present in the OC5 Chl *a* study. These differences arise from using Chl *a* to define regions compared to NPP, which is computed from Chl *a*, PAR and photosynthetic parameters. The threshold baseline indicators of NPP have previously been determined in the k-mean regions (Tilstone et al., 2023) and we therefore used the same regions and time-series, to assess significant changes in each region and analyse which environmental variables are causing changes in the trends.

4.2 Is primary production increasing or decreasing in the North Atlantic Ocean?

The requirements for estimating primary production from satellite to produce long time-series, are that it is retrievable from satellite parameters alone of the same duration, to be able to model at the same resolution, the light field, phytoplankton biomass, and photosynthesis parameters and that model variants should conform to the same basic formulation, with the same set of parameters (Brewin et al., 2021). The principal difficulty in modelling primary production from space is the assignment of the photosynthetic parameters on a per pixel basis (Sathyendranath et al., 2020). One of the key challenges in development of satellite estimates of NPP is that model parameters represent the spatial and temporal variability in photosynthetic rates (Brewin et al., 2023). A recent review of satellite derived NPP (and gross primary production GPP) models (Westberry et al., 2023), described how early NPP model approaches pioneered the parameterisation of the submarine light field throughout the day, and accounted for diffuse and direct components of sunlight, as well as dealing with non-uniformity of the Chl *a* profile in the water column (Platt and

TABLE 1 Least squares linear regression metrics of annual net primary production in north-east Atlantic regions from 1997 to 2018. The first column gives the region, the other columns give the statistical metrics. P value is the level of significance determined using a two-tailed t-test, R^2 is the variance explained, RMSE is root mean square error, N is the number of data points used.

Region	P value	R^2	RMSE	Slope	Slope std error	Intercept	Intercept std error	N
10. North Atlantic	0.0002	0.95	0.06	−0.0002	0.0023	0.47	4.65	21
9. Central Norwegian Sea	0.0004	0.94	0.04	−0.0001	0.0013	0.53	2.70	21
6. Northern North Sea	0.0107	0.65	0.03	−0.0004	0.0009	0.54	1.87	21
1. Irish Sea	0.0162	0.58	0.04	−0.0007	0.0013	0.85	2.56	21
3. Western English Channel	0.0170	0.57	0.03	−0.0006	0.0011	0.68	2.22	21
5. Kattegat and south-east North Sea	0.0229	0.51	0.06	−0.0005	0.0023	1.01	4.52	21
8. Faroe-Shetland channel	0.0235	0.51	0.05	−0.0012	0.0017	0.62	3.45	21
−1. All regions	0.0274	0.47	0.03	−0.0009	0.0013	0.63	2.51	21
2. North-west European coast	0.0300	0.45	0.12	−0.0034	0.0044	1.44	8.82	21
0. Celtic Sea	0.0316	0.44	0.02	0.0007	0.0009	0.53	1.78	21
4. Southern North Sea & Skagerrak	0.0894	0.19	0.03	−0.0013	0.0009	0.93	1.90	21
7. North-east Atlantic	0.1326	0.10	0.05	−0.0028	0.0016	0.51	3.28	21

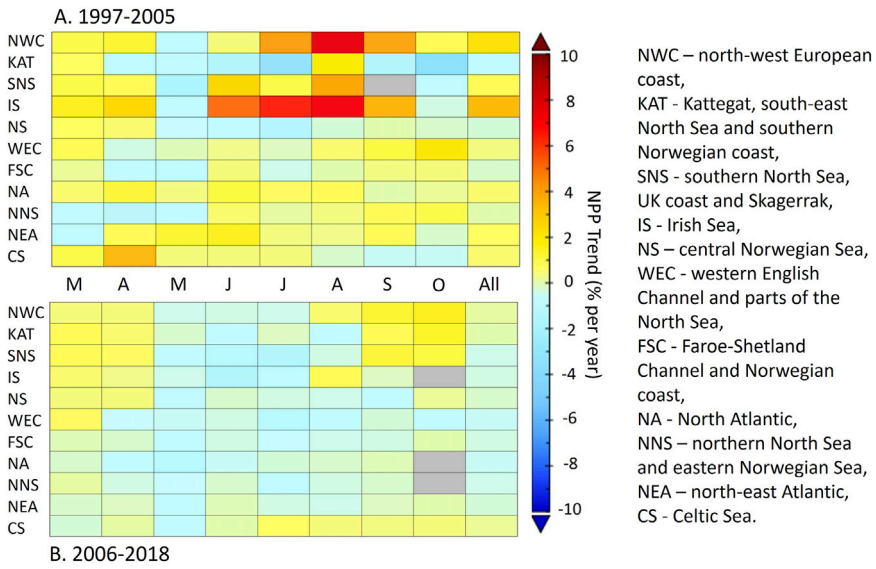

FIGURE 4
Regional and seasonal (March to October) significant relative trend in net primary production for the periods **(A)** 1997–2005 and **(B)** 2006–2018 for areas in the north-east Atlantic. Columns represent the different months (from M = March to O=October; All is all months from March to October). Rows represent the different regions. The scale bar is trend in NPP as % per year, where warm colours indicate an increase and cold colours indicate a decrease in NPP. Grey indicates no significant trend.

TABLE 2 **Significant (two-tailed t-test, 5% significance) least squares linear regressions between mean annual NPP and environmental variables for north-eastern Atlantic Ocean regions from 1997 to 2018. The first column gives the region, the other columns give the statistical metrics. R^2 is the variance explained, RMSE is root mean square error, Slope SE is the standard error in the slope, N is the number of data points used.**

Region	Variable A	Variable B	R^2	RMSE	Intercept	Slope A	Slope B	Intercept std error	Slope SE A	Slope SE B	N
5. Kattegat	SST	mld	0.45	0.011	0.0004	0.0609	0.0417	0.0007	0.0043	0.0025	244
6. Northern North Sea	mld	SST	0.25	0.007	0.0000	0.0339	0.0134	0.0004	0.0039	0.0015	244
2. North-west European coast	mld	NAO	0.25	0.014	0.0003	−0.0728	0.0493	0.0009	0.0081	0.0017	244
1. Irish Sea	SST	Mwind	0.21	0.008	0.0000	0.0616	0.0066	0.0005	0.0083	0.0025	244
3. Western English Channel	SST		0.17	0.006	0.0000	0.0419		0.0004	0.0059		244
10. North Atlantic	Zwind	SST	0.16	0.016	0.0004	0.0821	−0.0007	0.0010	0.0135	0.0003	244
−1. All regions	SST		0.15	0.006	0.0001	0.0444		0.0004	0.0067		244
4. Skagerrak	NAO	SST	0.13	0.007	0.0000	0.0291	0.0062	0.0005	0.0051	0.0026	244
8. Faroe-Shetland	SST	Mwind	0.13	0.010	0.0002	0.0517	0.0077	0.0006	0.0087	0.0029	244
9. Central Norwegian Sea	SST		0.11	0.014	0.0002	0.0495	0.0078	0.0009	0.0107	0.0029	244

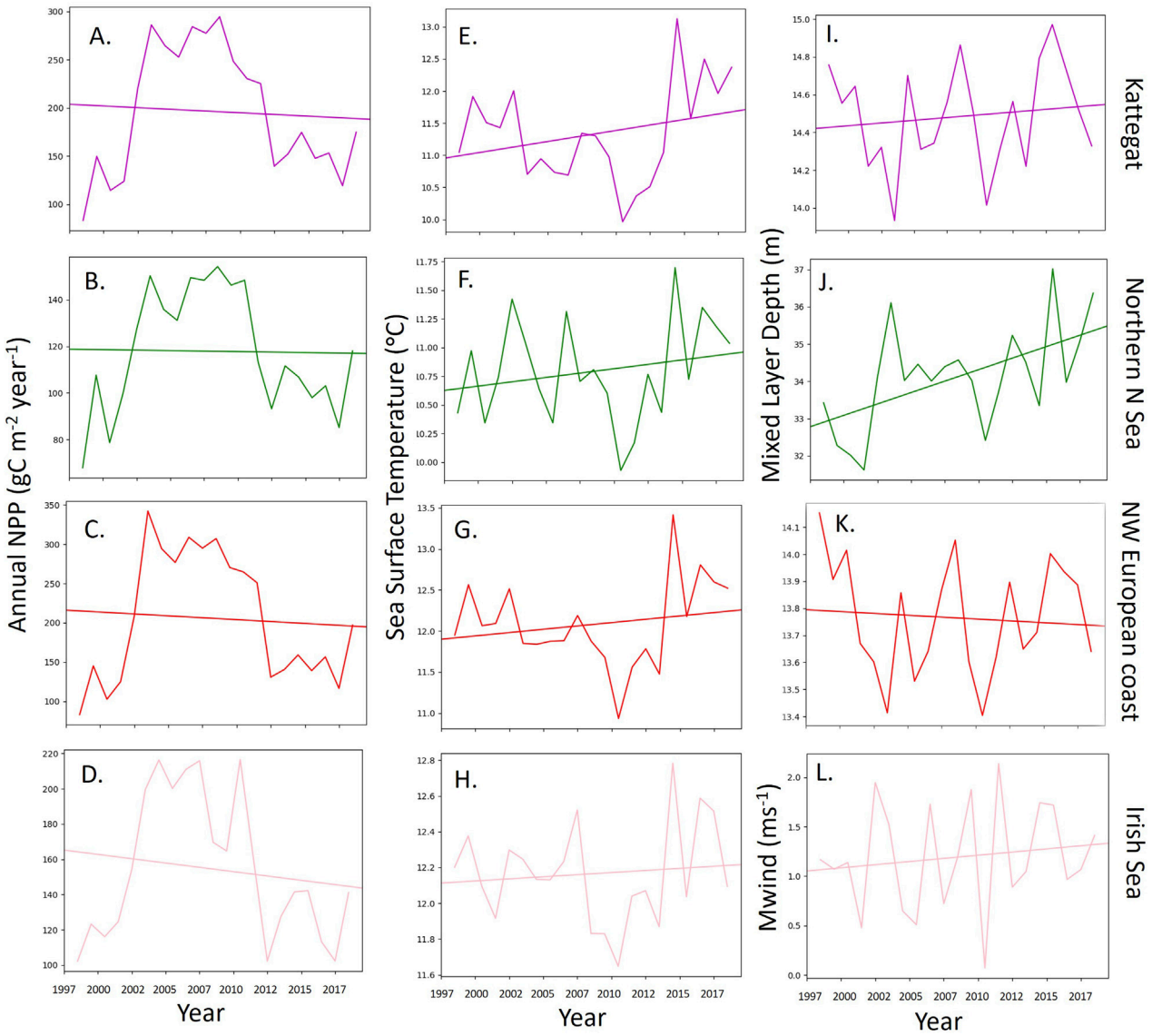

FIGURE 5
Regional trends in NPP most strongly correlated (highest r^2) with environmental variables. NPP trends are in the left column and the corresponding trends in environmental variables are in the middle and right columns as follows; Trends in annual NPP for **(A)** Kattegat, **(B)** northern North Sea, **(C)** north-west European coast **(D)** Irish Sea; in sea surface temperature (SST) in the **(E)** Kattegat, **(F)** northern North Sea, **(G)** north-west European coast **(H)** Irish Sea; in mixed layer depth (MLD) in the **(I)** Kattegat, **(J)** northern North Sea, **(K)** north-west European coast; and in meridional wind (mwind) in the **(L)** Irish Sea.

Sathyendranath, 1988; Morel, 1991). Updates on these seminal models, included re-computation of the light field by accounting for the absorption of light by Coloured Dissolved and detrital Matter (CDM) (Smyth et al., 2005; Silsbe et al., 2016), so that the models are more accurate and fit for purpose for use in coastal areas (Tilstone et al., 2005).

With increasing anthropogenic CO_2 emissions, global NPP is projected to decrease slightly to moderately by the end of the 21st century (Bopp et al., 2013; Riahi et al., 2011; Stock et al., 2014), primarily due to nutrient limitation resulting from enhanced surface-ocean stratification (Doney, 2006). Based on the first decade of quantitative satellite ocean colour observations, NPP decreased globally (Behrenfeld et al., 2006; Boyce et al., 2010). Using two decades of ocean colour observations from 1997 to 2018, NPP continued to decrease from 2011 until 2015, but the changes were not significant (Kulk et al., 2020). There have been a wide range of studies on long term trends in Chl *a*. NPP however is not only controlled by Chl *a*, but also by photosynthetic rates and the water column light field, which means that it can vary more than Chl *a* (Falkowski et al., 1998). It is therefore more sensitive to environmental changes and may not always track the trend in Chl *a* (Tilstone et al., 2023).

Few studies have used OC-CCI to compute NPP and assessed trends in the time-series. Lobanova et al. (2018) compared the performance of different optical models of NPP using OC-CCI v3. Zvalinsky et al. (2019) used *in situ* and satellite derived NPP from

OC-CCI v2 to assess the variability of NPP in the north-west Pacific around Japan. Frolova et al. (2023) used OC-CCI v6 to assess trends in NPP from 2003 to 2022 over the Arctic Ocean, which increased by 18.5%, and showed a larger increase in the Laptev Sea (by 32%) but decreased in the Chukchi Sea by 13.6%. A more recent study compared five NPP algorithms using OC-CCI v6 (Ryan-Koegh et al.,. 2023). Trends in NPP over 23 years of OC-CCI were compared at four point stations (BATS, HOTS, PAP and SOTS), but not at global, basin or regional scales. Upward or downward trends were observed in NPP, depending on the model used (Ryan-Koegh et al.,. 2023). All of these studies used or included the vertical general production model (VGPM), which is known to overestimate and have large bias in NPP (Carr et al., 2006; Saba et al., 2011; Tilstone et al., 2009) due to errors in irradiance-depth dependent and photosynthetic rate functions (Milutinovic and Bertino, 2011; Tilstone et al., 2015).

Kulk et al. (2020) used a WRM NPP model with OC-CCI v4.1 data, and observed an increase in NPP, globally and in the Atlantic Ocean, from 1998 to 2003, and a subsequent decrease from 2011 to 2015. For comparability with Kulk et al. (2020), we also utilised a WRM with OC-CCI v4 to compute NPP. Global or basin scale trends in NPP do not necessarily reflect those at finer hydrographic scales (Steinacher et al., 2010; Rykaczewski and Dunne, 2010), and it is important to evaluate these in relation to localised atmospheric dynamics and terrestrial input that can cause variations in NPP to provide deeper understanding of how these vary at basin or regional scales. We therefore analysed trends in NPP over the same time period and using the same satellite OC-CCI v4 data as Kulk et al. (2020), but at a finer scale in the north-east Atlantic and observed that many of the regions analysed exhibited a significant decrease in NPP (Figure 3; Table 1), which varied between regions.

In coastal regions of the North Atlantic the scenario can be very different to the open ocean due to the influence of riverine run-off. In the North Sea, an increase in NPP and changes in phytoplankton species composition from the 1960s until the 1980s have been related to increases in riverine nitrogen, which in some areas led to hypoxia (Patsch and Radach, 1997; Philippart and Cadée, 2000; 2007). Similarly, off the coast of Sweden at the entrance to the Gullmar Fjord, Tiselius et al. (2016) reported an increase in NPP from 1985 to 1995, with a subsequent decline due to high grazing by zooplankton. In the eastern English Channel Gohin et al. (2019) reported a decline in CMEMS ocean colour Chl *a* over the past 20 years in the eastern English Channel linked to a reduction in riverine phosphate to the coastal zone. Similarly, from our data in north-west European coastal waters we observed a decline in NPP from 2002 to 2017 (Figure 5C).

4.3 Environmental forcing of primary production in the North Atlantic Ocean

It is essential to understand why NPP varies over specific regions, why it is shifting over time and the principal environmental forcing factors for these. In our analysis, SST was one of the principal factors that varied with NPP, as well as MLD (Table 2). We found that an increase in NPP over the north-east Atlantic up to 2004 was positively correlated with SST. After this period, NPP continued to decrease to 2018 (Figure 3, 5). The historical context of this is that in the 1970s and early 1980s there was a cold period in the North Atlantic, which reduced the Atlantic inflow to the north-east Atlantic, causing a decline in NPP and geographical changes in zooplankton communities (Drinkwater and Kristiansen, 2018). Stratification of the water column has increased globally over the period from 1971 to 2010 by 4% (Li et al., 2020). By contrast, in the north-east Atlantic a negative correlation between SST and NPP was recorded (Richardson and Schoeman, 2004). Positive or non-linear relationships between SST and phytoplankton were also reported in the North Sea (Llope et al., 2009) and the North Atlantic (Irwin and Finkel, 2008).

We observed a decline in NPP in the southern, central and northern North Sea, the Kattegat and Irish Sea over the 21-year time series, which were positively correlated with increases in SST and MLD (Table 2; Figure 5). A decline in NPP in the southern North Sea from 1988 to 2013 was also reported by Capuzzo et al. (2018), who related this to a reduction in water clarity resulting from an increase in SPM (Capuzzo et al., 2015). This was caused by a significant increase in bed shear stress from 1997 to 2017, arising from greater waves and currents (Wilson and Heath, 2019), resulting in higher MLDs. In our study, SST increases during spring, summer and autumn, as shown in Figure 5, and stratification predominates. Over this period however, there can be periodic increases in wind speed, which cause a deepening of the MLD, an increase in bed shear stress and SPM as observed by Wilson and Heath (2019) and Capuzzo et al. (2015), resulting in a reduction in light available for photosynthesis and a reduction in NPP. In the northern hemisphere, a poleward shift in the jet stream results in changes in wind fields (Lauderdale et al., 2013; Landschützer et al., 2015) that impact the upper ocean vertical structure and circulation (Somavilla et al., 2016), resulting in variable MLD and stratification over local regions. At mid-latitudes however, though SST is increasing, there is little evidence of increased stratification or lower MLD (Somavilla et al., 2017). The seasonal shift in NPP from May to March-April may also be related to an earlier shoaling of the MLD and entrainment of nutrients and phytoplankton in the upper euphotic zone earlier from winter to spring (Sverdrup, 1957). The change from increasing to decreasing NPP trends from July-August to September-October in the north-west European coast, southern North Sea and Irish Sea that we observed, is likely to be due to prolonged surface stratification and shallower mixed layers during summer until autumn (Lozier et al., 2011). At the global scale the reported decrease in satellite NPP by Gregg and Rousseaux (2019) was seen to be due to a shallowing of the MLD and a decrease in nitrate concentrations. In the open ocean, the decrease in marine productivity may be associated with a deepening of the phosphate maxima causing phosphate limitation, rather than nitrate limitation *per se* (Gerace et al., 2025).

4.4 Potential impacts of shifts in net primary production in the North Atlantic Ocean

In our study, the highest decrease in NPP was in the north-west European coast and north-east Atlantic, and the lowest was in the central Norwegian Sea, North Atlantic and northern North Sea. In the Celtic Sea, NPP actually increased over this period (Figure 3; Table 1). Furthermore, on a seasonal basis, the localised pattern in NPP shifted (Figure 4). The trend maps in Figure 4 indicate that from March to April, the NPP trend changed from positive to

negative in 1997–2005 in the Kattegat, western English Channel and Faroe-Shetland Channel, and in 2006–2018 in the western English Channel, while in 1997–2005 in the north-east Atlantic region the trend changed from negative to positive, and the positive trend in the Celtic Sea strongly increased.

The implications of these trends are that the reduction and seasonal shift in NPP could alter the energy transfer to higher trophic levels, especially in the north-west European coast and north-east Atlantic regions, where the decrease in NPP is most acute. This could potentially impact local fisheries (Free, 2019). The shift in the spring NPP peak from May to March-April and the reduction in NPP during May especially in the Kattegat, western English Channel and Faroe-Shetland Channel, could further impact fisheries with implications for food security. For those regions that do not show a decline in NPP, such as the Celtic Sea, there may be increased feeding pressure from fish and mammals from surrounding areas experiencing a decline in NPP, such as the north-east Atlantic, Irish Sea and western English Channel, as they migrate in search of food. Similarly, for those regions experiencing the highest decrease in NPP there may be local alteration in the ocean's biological pump and decrease in export production, which could alter the regional uptake of CO_2 and impact the food supply to both pelagic and benthic habitats and regional ecosystem services. Shifts to an early peak in NPP have been predicted in the northern domain of the North Atlantic due to an earlier shoaling of the MLD, which will affect zooplankton and larvae as the timing of available food resources occurs earlier (Hieronymus et al., 2024). The length of the current ocean colour record is too short to assess the regional impact of climate change on NPP, but with consistent support by the space agencies to ensure high quality ocean colour data over the next decade, an assessment of climate change effects on NPP will be possible. For the north-east Atlantic, these varying patterns in NPP reflect the complexity at the sub-regional scale, which has implications on the capacity of regional seas to regulate the climate and need to be considered when assessing global and basin scale trends in NPP.

5 Conclusions

A 21-year time series of primary production from 1997 to 2018 was computed using a wavelength resolving NPP model and 4 km OC-CCI data for the north-east Atlantic. Over the whole study area, NPP increased from 1997 to 2003, and then decreased from 2005 to 2018, with an overall net decrease. K-means cluster analysis based on similarity in NPP timing, phenology and annual rates was used to assess the variability in NPP at sub-regional scales. For the north-east Atlantic, most sub-regions exhibited a significant decrease in NPP which for some regions was related to an increase in SST and either a decrease or an increase in MLD. This study illustrates the complexity of localised heating, wind regimes and MLD and their effect on NPP, which should be considered in the context of global and basin scale trends in NPP. The regional reduction and seasonal shift in NPP, especially in the north-west European coast and north-east Atlantic sub-regions, has implications for altering the energy transfer to higher trophic levels and altering the uptake of CO_2 by regional seas, both of which could potentially impact ecosystem services.

Data availability statement

The raw data supporting the conclusions of this article will be made available by the authors, without undue reservation.

Author contributions

GT: Conceptualization, Funding acquisition, Investigation, Project administration, Resources, Supervision, Writing – original draft, Writing – review and editing. PL: Data curation, Formal Analysis, Investigation, Methodology, Software, Validation, Visualization, Writing – review and editing.

Funding

The author(s) declared that financial support was received for this work and/or its publication. The research was funded by NEA PANACEA (North-East Atlantic project on biodiversity and eutrophication assessment integration and creation of effective measures) from the European Commission DG Environment/ Marine Strategy Framework Directive 2020 (Contract number 31167499) and also funded by The Western Channel Observatory funded by the United Kingdom Natural Environment Research Council through its National Capability Long-term Single Centre Science Programme, Atlantic Climate and Environment Strategic Science (AtlantiS; grant number NE/Y005589/1).

Acknowledgements

Ocean colour imagery was provided by the Ocean Colour Climate Change Initiative (OC-CCI) funded by the European Space Agency and produced by Andrei Chuprin, Plymouth Marine Laboratory. We are grateful to NEODAAS for hosting the data and allowing us computing capacity to process the NPP images.

Conflict of interest

The author(s) declared that this work was conducted in the absence of any commercial or financial relationships that could be construed as a potential conflict of interest.

Generative AI statement

The author(s) declared that generative AI was not used in the creation of this manuscript.

Any alternative text (alt text) provided alongside figures in this article has been generated by Frontiers with the support of artificial intelligence and reasonable efforts have been made to ensure accuracy, including review by the authors wherever possible. If you identify any issues, please contact us.

Publisher's note

References

Barnston, A. G., and Livezey, R. E. (1987). Classification, seasonality and persistence of low-frequency atmospheric circulation patterns. *Mon. Weather Rev.* 115 (6), 1083–1126. doi:10.1175/1520-0493(1987)115<1083:csapol>2.0.co;2

Bates, N. R. (2017). Twenty years of marine carbon cycle observations at Devils Hole Bermuda provide insights into seasonal hypoxia, coral reef calcification, and ocean acidification. *Front. Mar. Sci.* 4, 36. doi:10.3389/fmars.2017.00036

Beardall, J., Sobrino, C., and Stojkovic, S. (2009). Interactions between the impacts of ultraviolet radiation, elevated CO2, and nutrient limitation on marine primary producers. *Photochem. & Photobiological Sci.* 8 (9), 1257–1265. doi:10.1039/b9pp00034h

Behrenfeld, M. J., O'Malley, R. T., Siegel, D. A., McClain, C. R., Sarmiento, J. L., Feldman, G. C., et al. (2006). Climate-driven trends in contemporary ocean productivity. *Nature* 444 (7120), 752–755. doi:10.1038/nature05317

Blauw, A., Aumont, O., and Dufresne, J. (2019). Coherence in assessment framework of chlorophyll a and nutrients as part of the EU project 'Joint monitoring programme of the eutrophication of the North Sea with satellite data' (ref: DG ENV/MSFD second Cycle/ 2016). Available online at: https://www.informatiehuismarien.nl/publish/pages/163016/ 1_coherent_assessment (Accessed December 05, 2026).

Bopp, L., Resplandy, L., Orr, J. C., Doney, S. C., Dunne, J. P., Gehlen, M., et al. (2013). Multiple stressors of ocean ecosystems in the 21st century: projections with CMIP5 models. *Biogeosciences* 10 (10), 6225–6245. doi:10.5194/bg-10-6225-2013

Boyce, D. G., Lewis, M. R., and Worm, B. (2010). Global phytoplankton decline over the past century. *Nature* 466 (7306), 591–596. doi:10.1038/nature09268

Brewin, R. J. W., Sathyendranath, S., Platt, T., Bouman, H., Ciavatta, S., Dall'Olmo, G., et al. (2021). Sensing the ocean biological carbon pump from space: a review of capabilities, concepts, research gaps and future developments. *Earth-Science Rev.* 217, 103604. doi:10.1016/j.earscirev.2021.103604

Brewin, R. J. W., Sathyendranath, S., Kulk, G., Rio, M. H., Concha, J. A., Bell, T. G., et al. (2023). Ocean carbon from space: current status and priorities for the next decade. *Earth-Science Rev.* 240, 104386. doi:10.1016/j.earscirev.2023.104386

Campbell, J., Antoine, D., Armstrong, R., Arrigo, K., Balch, W., Barber, R., et al. (2002). Comparison of algorithms for estimating ocean primary production from surface chlorophyll, temperature, and irradiance. *Glob. Biogeochem. Cycles* 16 (3), 1035. doi:10.1029/2001gb001444

Capuzzo, E., Stephens, D., Silva, T., Barry, J., and Forster, R. M. (2015). Decrease in water clarity of the southern and central north sea during the 20th century. *Glob. Change Biol.* 21 (6), 2206–2214. doi:10.1111/gcb.12854

Capuzzo, E., Lynam, C. P., Barry, J., Stephens, D., Forster, R. M., Greenwood, N., et al. (2018). A decline in primary production in the north sea over 25 years, associated with reductions in zooplankton abundance and fish stock recruitment. *Glob. Change Biol.* 24 (1), E352–E364. doi:10.1111/gcb.13916

Carr, M. E., Friedrichs, M. A., Schmeltz, M., Noguchi Aita, M., Antoine, D., Arrigo, K. R., et al. (2006). A comparison of global estimates of marine primary production from ocean color. *Deep-Sea Res. Part II-Topical Stud. Oceanogr.* 53, 741–770. doi:10.1016/j.dsr2.2006.01.028

Chavez, F. P., Messié, M., and Pennington, J. T. (2011). Marine primary production in relation to climate variability and change. *Annu. Rev. Mar. Sci.* 3, 227–260. doi:10.1146/annurev.marine.010908.163917

CMEMS Global Ocean Ensemble Physics Reanalysis. E.U. (2022). Copernicus marine service information. *Mar. Data Store (MDS).* doi:10.48670/moi-00024

Devlin, M. J., Prins, T. C., Enserink, L., Leujak, W., Heyden, B., Axe, P. G., et al. (2023). A first ecological coherent assessment of eutrophication across the North-East Atlantic waters (2015–2020). *Front. Ocean Sustain.* 1, 1253923. doi:10.3389/focsu.2023.1253923

Doney, S. C. (2006). Oceanography - Plankton in a warmer world. *Nature* 444 (7120), 695–696. doi:10.1038/444695a

Drinkwater, K. F., and Kristiansen, T. (2018). A synthesis of the ecosystem responses to the late 20th century cold period in the northern north Atlantic. *Ices J. Mar. Sci.* 75 (7), 2325–2341. doi:10.1093/icesjms/fsy077

D'Alelio, D., Rampone, S., Cusano, L. M., Morfino, V., Russo, L., Sanseverino, N., et al. (2020). Machine learning identifies a strong association between warming and reduced primary productivity in an oligotrophic ocean gyre. *Sci. Rep.* 10, 1–12. doi:10.1038/s41598-020-59989-y

Falkowski, P. G., Barber, B., and Smetacek, S. (1998). Biogeochemical controls and feed backs on ocean primary production. *Science* 281, 200–206. doi:10.1126/science.281.5374.200

Falkowski, P. G., Katz, M. E., Knoll, A. H., Quigg, A., Raven, J. A., Schofield, O., et al. (2004). The evolution of modern eukaryotic phytoplankton. *Science* 305 (5682), 354–360. doi:10.1126/science.1095964

Field, C. B., Behrenfeld, B., Randerson, R., and Falkowski, F. (1998). Primary production of the biosphere: integrating terrestrial and Oceanic components. *Science* 281 (5374), 237–240. doi:10.1126/science.281.5374.237

Ford, D., Tilstone, G. H., Shutler, J. D., Kitidis, V., Lobanova, P., Schwarz, J., et al. (2021). Wind speed and mesoscale processes drive net autotrophy in the south Atlantic Ocean. *Remote Sens. Env.* 260, 112435. doi:10.1016/j.rse.2021.112435

Free, F. M., Thorson, J. T., Pinsky, M. L., Oken, K. L., Wiedenmann, J., and Jensen, O. P. (2019). Impacts of historical warming on marine fisheries production. *Science* 363, 979–983. doi:10.1126/science.aau1758

Friedrichs, M. A. M., Carr, M. E., Barber, R. T., Scardi, M., Antoine, D., Armstrong, R. A., et al. (2009). Assessing the uncertainties of model estimates of primary productivity in the tropical Pacific Ocean. *J. Mar. Syst.* 76, 113–133. doi:10.1016/j.jmarsys.2008.05.010

Frolova, A. V., Morozov, E. A., and Pozdnyakov, D. V. (2023). The Arctic Ocean primary production in response to amplification of climate change: insights from 2003-2022 satellite data. *Izvestiya Atmos. Ocean. Phys.* 59 (10), 1450–1458. doi:10.1134/s0001433823120095

Gerace, S. D., Yu, J., Moore, J. K., and Martiny, A. C. (2025). Observed declines in upper ocean phosphate-to- nitrate availability. *Proc. Natl. Acad. Sci. U. S. A.* 122 (6), e2411835122. doi:10.1073/pnas.2411835122

Gohin, F., Druon, J. N., and Lampert, L. (2002). A five channel chlorophyll concentration algorithm applied to SeaWiFS data processed by SeaDAS in coastal waters. *Int. J. Remote Sens.* 23 (8), 1639–1661. doi:10.1080/01431160110071879

Gohin, F., Van der Zande, D., Tilstone, G., Eleveld, M. A., Lefebvre, A., Andrieux-Loyer, F., et al. (2019). Twenty years of satellite and *in situ* observations of surface chlorophyll-a from the northern Bay of Biscay to the eastern English Channel. Is the water quality improving? *Remote Sens. Environ.* 233, 111343. doi:10.1016/j.rse.2019.111343

Gregg, W. W., and Carder, K. L. (1990). A simple spectral solar irradiance model for cloudless maritime atmospheres. *Limnol. Oceanogr.* 35, 1657–1675. doi:10.4319/lo.1990.35.8.1657

Gregg, W. W., and Rousseaux, C. S. (2019). Global ocean primary production trends in the modern ocean color satellite record (1998–2015). *Environ. Res. Lett.* 14 (12), 124011. doi:10.1088/1748-9326/ab4667

Henson, S. A., Sarmiento, J. L., Dunne, J. P., Bopp, L., Lima, I., Doney, S. C., et al. (2010). Detection of anthropogenic climate change in satellite records of ocean chlorophyll and productivity. *Biogeosciences* 7 (2), 621–640. doi:10.5194/bg-7-621-2010

Hersbach, H., Bell, B., Berrisford, P., Biavati, G., Horányi, A., Muñoz Sabater, J., et al. (2023). ERA5 hourly data on single levels from 1940 to present. *Copernic. Clim. Change Serv. (C3S) Clim. Data Store (CDS).*

Hieronymus, J., Hieronymus, M., Gröger, M., Schwinger, J., Bernadello, R., Tourigny, E., et al. (2024). Net primary production annual maxima in the north Atlantic projected to shift in the 21st century. *Biogeosciences* 21, 2189–2206. doi:10.5194/bg-21-2189-2024

Hubert, L. J., and Levin, J. R. (1976). A general statistical framework for assessing categorical clustering in free recall. *Psychol. Bull.* 83 (6), 1072–1080. doi:10.1037/0033-2909.83.6.1072

Irwin, A. J., and Finkel, Z. V. (2008). Mining a sea of data: deducing the environmental controls of ocean chlorophyll. *Plos One* 3 (11), e3836. doi:10.1371/journal.pone.0003836

Jackson, T., Volpe, G., Sathyendranath, S., and Groom, S. (2021). ESA ocean colour climate change initiative – phase 3: product validation and intercomparison report (plymouth). *Plymouth Mar. Laboratory (PML) ESA Clim. Office*, 1–17. Available online at: https://climate.esa.int (Accessed December 5, 2026).

Kulk, G., Platt, T., Dingle, J., Jackson, T., Jönsson, B., Bouman, H., et al. (2020). Primary production, an index of climate change in the ocean: satellite-based estimates over two decades. *Remote Sens.* 12 (5), 826. doi:10.3390/rs12050826

Landschützer, P., Gruber, N., Haumann, F. A., Rödenbeck, C., Bakker, D. C. E., van Heuven, S., et al. (2015). The reinvigoration of the Southern Ocean carbon sink. *Science* 349 (6253), 1221–1224. doi:10.1126/science.aab2620

Lauderdale, J. M., Garabato, A. C. N., Oliver, K. I. C., Follows, M. J., and Williams, R. G. (2013). Wind-driven changes in Southern Ocean residual circulation, ocean carbon reservoirs and atmospheric CO2. *Clim. Dyn.* 41 (7-8), 2145–2164. doi:10.1007/s00382-012-1650-3

Lavigne, H., Van der Zande, D., Ruddick, K., Cardoso Dos Santos, J., Gohin, F., Brotas, V., et al. (2021). Quality-control tests for OC4, OC5 and NIR-Red satellite chlorophyll-a algorithms applied to coastal waters. *Remote Sens. Environ.* 255, 112237. doi:10.1016/j.rse.2020.112237

Lee, Y. J., Matrai, P. A., Friedrichs, M. A. M., Saba, V. S., Antoine, D., Ardyna, M., et al. (2015). An assessment of phytoplankton primary productivity in the Arctic Ocean from satellite ocean color/in situ chlorophyll-a based models. *J. Geophys. Res. Oceans* 120, 6508–6541. doi:10.1002/2015JC011018

Lee, Z., and Hu, C. (2006). Global distribution of Case-1 waters: an analysis from SeaWiFS measurements. *Remote Sens. Environ.* 101 (2), 270–276. doi:10.1016/j.rse.2005.11.008

Li, G., Cheng, L., Zhu, J., Trenberth, K. E., Mann, M. E., and Abraham, J. P. (2020). Increasing ocean stratification over the past half-century. *Nat. Clim. Chang.* 10, 1116–1123. doi:10.1038/s41558-020-00918-2

Llope, M., Chan, K. S., Ciannelli, L., Reid, P. C., Stige, L. C., and Stenseth, N. C. (2009). Effects of environmental conditions on the seasonal distribution of phytoplankton biomass in the north sea. *Limnol. Oceanogr.* 54 (2), 512–524. doi:10.4319/lo.2009.54.2.0512

Lobanova, P., Tilstone, G. H., Bashmachnikov, I., and Brotas, V. (2018). Accuracy assessment of primary production models with and without photoinhibition using ocean-colour climate change initiative data in the north east Atlantic Ocean. *Remote Sens.* 10 (7), 1116. doi:10.3390/rs10071116

Lomas, M. W., Steinberg, D. K., Dickey, T., Carlson, C. A., Nelson, N. B., Condon, R. H., et al. (2010). Increased ocean carbon export in the Sargasso Sea linked to climate variability is countered by its enhanced mesopelagic attenuation. *Biogeosciences* 7 (1), 57–70. doi:10.5194/bg-7-57-2010

Lomas, M. W., Bates, N., Johnson, R., Knap, A., Steinberg, D., and Carlson, C. (2013). Two decades and counting: 24-years of sustained open ocean biogeochemical measurements in the Sargasso Sea. *Deep-Sea Res. Part Ii-Topical Stud. Oceanogr.* 93, 16–32. doi:10.1016/j.dsr2.2013.01.008

Lomas, M. W., Bates, N. R., Johnson, R. J., Steinberg, D. K., and Tanioka, T. (2022). Adaptive carbon export response to warming in the Sargasso Sea. *Nat. Commun.* 13, 1211. doi:10.1038/s41467-022-28842-3

Lozier, M. S., Dave, A. C., Palter, J. B., Gerber, L. M., and Barber, R. T. (2011). On the relationship between stratification and primary productivity in the North Atlantic. *Geophys. Res. Lett.* 38, L18609. doi:10.1029/2011gl049414

McGillicuddy, D. J., Robinson, A. R., Siegel, D. A., Jannasch, H. W., Johnson, R., Dickey, T. D., et al. (1998). Influence of mesoscale eddies on new production in the Sargasso Sea. *Nature* 394 (6690), 263–266. doi:10.1038/28367

Mélin, F., Vantrepotte, V., Chuprin, A., Grant, M., Jackson, T., and Sathyendranath, S. (2017). Assessing the fitness-for-purpose of satellite multi-mission ocean color climate data records: a protocol applied to OC-CCI chlorophyll-a data. *Remote Sens. Environ.* 203, 139–151. doi:10.1016/j.rse.2017.03.039

Milutinovic, S., and Bertino, L. (2011). Assessment and propagation of uncertainties in input terms through an ocean-color-based model of primary productivity. *Remote Sens. Environ.* 115, 1906–1917. doi:10.1016/j.rse.2011.03.013

Morel, A., Antoine, D., Babin, M., and Dandonneau, Y. (1996). Measured and modeled primary production in the northeast Atlantic (EUMELI JGOFS program): the impact of natural variations in photosynthetic parameters on model predictive skill. *Deep-Sea Research I*43, 1273–1304. doi:10.1016/0967-0637(96)00059-3

Morel, A. (1991). Light and marine photosynthesis - a spectral model with geochemical and climatological implications. *Prog. Oceanogr.* 26 (3), 263–306. doi:10.1016/0079-6611(91)90004-6

Morel, A. (1988). Optical modelling of the upper ocean in relation to its biogenous matter content (Case I waters). *J. Geophys. Res.* 93, 10749–10768. doi:10.1029/JC093iC09p10749

Morel, A., and Berthon, J. F. (1989). Surface pigments, algal biomass profiles, and potential production of the euphotic layer—Relationships reinvestigated in view of remote sensing applications. *Limnol. Oceanogr.* 34, 1545–1562. doi:10.4319/lo.1989.34.8.1545

Novoa, S., Chust, G., Sagarminaga, Y., Revilla, M., Borja, A., and Franco, J. (2012). Water quality assessment using satellite-derived chlorophyll-a within the European directives, in the southeastern Bay of Biscay. *Mar. Pollut. Bull.* 64 (4), 739–750. doi:10.1016/j.marpolbul.2012.01.020

O'Reilly, J. E., Beukema, J. J., and Cadée, G. C. (2000). "Ocean color chlorophyll-a algorithms for SeaWiFS, OC2 and OC4: version 4," in *SeaWiFS postlaunch technical report series 11 SeaWiFS postlaunch calibration and validation analyses*. Editors S. B. Hooker and E. R. Firestone, 3, 9–23.

Patsch, J., and Radach, G. (1997). Long-term simulation of the eutrophication of the north sea: temporal development of nutrients, chlorophyll and primary production in comparison to observations. *J. Sea Res.* 38 (3-4), 275–310. doi:10.1016/s1385-1101(97)00051-8

Philippart, C. J. M., and Cadée, G. C. (2000). Was total primary production in the Western Wadden Sea stimulated by nitrogen loading? *Helgol. Mar. Res.* 54 (2-3), 55–62. doi:10.1007/s101520050002

Philippart, C. J. M., Beukema, J. J., Cadée, G. C., Dekker, R., Goedhart, P. W., van Iperen, J. M., et al. (2007). Impacts of nutrient reduction on coastal communities. *Ecosystems* 10 (1), 95–118. doi:10.1007/s10021-006-9006-7

Platt, T., and Sathyendranath, S. (1988). Oceanic primary production: estimation by remote sensing at local and regional scales. *Science* 241, 1613–1620. doi:10.1126/science.241.4873.1613

Raven, J. A., Giordano, M., Beardall, J., and Maberly, S. C. (2012). Algal evolution in relation to atmospheric CO2: carboxylases, carbon-concentrating mechanisms and carbon oxidation cycles. *Philosophical Trans. R. Soc. B-Biological Sci.* 367 (1588), 493–507. doi:10.1098/rstb.2011.0212

Riahi, K., Rao, S., Krey, V., Cho, C., Chirkov, V., Fischer, G., et al. (2011). RCP 8.5-A scenario of comparatively high greenhouse gas emissions. *Clim. Change* 109 (1-2), 33–57. doi:10.1007/s10584-011-0149-y

Richardson, A. J., and Schoeman, D. S. (2004). Climate impact on plankton ecosystems in the north-east Atlantic. *Science* 305 (5690), 1609–1612. doi:10.1126/science.1100958

Robinson, C., Tilstone, G. H., Rees, A. P., Smyth, T. J., Fishwick, J. R., Tarran, G. A., et al. (2009). Comparison of *in vitro* and *in situ* plankton production determinations. *Aquat. Microb. Ecol.* 54, 13–34. doi:10.3354/ame01250

Robinson, A., Bouman, H. A., Tilstone, G. H., and Sathyendranath, S. (2018). Size class dependent relationships between temperature and phytoplankton photosynthesis-irradiance parameters in the Atlantic Ocean. *Front. Mar. Sci.* 4, 435. doi:10.3389/fmars.2017.00435

Ruddick, K. G., Gons, H. J., Rijkeboer, M., and Tilstone, G. (2001). Optical remote sensing of chlorophyll a in case 2 waters by use of an adaptive two-band algorithm with optimal error properties. *Appl. Opt.* 40 (21), 3575–3585. doi:10.1364/AO.40.003575

Ryan-Keogh, T. J., Thomalla, S. J., Chang, N., and Moalusi, T. (2023). A new global oceanic multi-model net primary productivity data product. *Earth Syst. Sci. Data* 15 (11), 4829–4848. doi:10.5194/essd-15-4829-2023

Rykaczewski, R. R., and Dunne, J. P. (2010). Enhanced nutrient supply to the California current ecosystem with global warming and increased stratification in an earth system model. *Geophys. Res. Lett.* 37, L21606. doi:10.1029/2010gl045019

Saba, V. S., Friedrichs, M. A. M., Carr, M.-E., Antoine, D., Armstrong, R. A., Asanuma, I., et al. (2010). Challenges of modeling depth-integrated marine primary productivity over multiple decades: a case study at BATS and HOT. *Glob. Biogeochem. Cycles* 24, GB3020. doi:10.1029/2009gb003655

Saba, V. S., Friedrichs, M. A. M., Antoine, D., Armstrong, R. A., Asanuma, I., Behrenfeld, M. J., et al. (2011). An evaluation of ocean color model estimates of marine primary productivity in coastal and pelagic regions across the globe. *Biogeosciences* 8, 489–503. doi:10.5194/bg-8-489-2011

Sathyendranath, S., Brewin, R. J. W., Brockmann, C., Brotas, V., Calton, B., Chuprin, A., et al. (2019). An ocean-colour time series for use in climate studies: the experience of the ocean-colour climate change initiative (OC-CCI). *Sensors* 19 (19), 4285. doi:10.3390/s19194285

Sathyendranath, S., Platt, T., Kovac, Z., Dingle, J., Jackson, T., Brewin, R. J. W., et al. (2020). Reconciling models of primary production and photoacclimation. *Appl. Opt.* 59, C100–C114. doi:10.1364/AO.386252

Saulquin, B., Gohin, F., and Garrello, R. (2011). Regional objective analysis for merging high-resolution MERIS, MODIS/Aqua, and SeaWiFS Chlorophyll-a data from 1998 to 2008 on the european Atlantic shelf. *Ieee Trans. Geoscience Remote Sens.* 49 (1), 143–154. doi:10.1109/tgrs.2010.2052813

Siemer, J. P., Machín, F., González Vega, A., Arrieta, J. M., Gutiérrez Guerra, M. A., Pérez-Hernández, M. D., et al. (2021). Recent trends in SST, Chl-a, productivity and wind stress in upwelling and open ocean areas in the upper eastern north Atlantic subtropical gyre. *J. Geophys. Res. Oceans* 126, e2021JC017268. doi:10.1029/2021jc017268

Silsbe, G. M., Behrenfeld, M. J., Halsey, K. H., Milligan, A. J., and Westberry, T. K. (2016). The CAFE model: a net production model for global ocean phytoplankton. *Glob. Biogeochem. Cycles* 30, 1756–1777. doi:10.1002/2016gb005521

Silsbe, G. M., Fox, J., Westberry, T. J., and Halsey, K. H. (2025). Global declines in primary production in the ocean color era. *Nat. Commun.* 16, 5821. doi:10.1038/s41467-025-60906-y

Smyth, T. J., Tilstone, G. H., and Groom, S. B. (2005). Primary production estimates from satellite data using a coupled radiative transfer – photosynthesis approach. *J. Geophys. Research-Oceans* 110, C10014. doi:10.1029/2004jc002784

Somavilla, R., González-Pola, C., Schauer, U., and Budéus, G. (2016). Mid-2000s north Atlantic shift: heat budget and circulation changes. *Geophys. Res. Lett.* 43 (5), 2059–2068. doi:10.1002/2015GL067254

Somavilla, R., González-Pola, C., and Fernández-Diaz, J. (2017). The warmer the ocean surface, the shallower the mixed layer. How much of this is true? *J. Geophys. Research-Oceans* 122 (9), 7698–7716. doi:10.1002/2017JC013125

Steinacher, M., Joos, F., Frölicher, T. L., Bopp, L., Cadule, P., Cocco, V., et al. (2010). Projected 21st century decrease in marine productivity: a multi-model analysis. *Biogeosciences* 7 (3), 979–1005. doi:10.5194/bg-7-979-2010

Stock, C. A., Dunne, J. P., and John, J. G. (2014). Drivers of trophic amplification of ocean productivity trends in a changing climate. *Biogeosciences* 11 (24), 7125–7135. doi:10.5194/bg-11-7125-2014

Sverdrup, H. U. (1957). On conditions for the vernal blooming of phytoplankton. *J. Cons. Cons. Int. Explor. Mer.* 18, 287–295. doi:10.1093/icesjms/18.3.287

Tilstone, G. H., Smyth, T. J., Gowen, R. J., Martinez-Vicente, V., and Groom, S. B. (2005). Inherent optical properties of the Irish sea and their effect on satellite primary production algorithms. *J. Plankton Res.* 27 (10), 1–22. doi:10.1093/plankt/fbi075

Tilstone, G., Smyth, T., Poulton, A., and Hutson, R. (2009). Measured and remotely sensed estimates of primary production in the Atlantic Ocean from 1998 to 2005. *Deep-Sea Res. Part Ii-Topical Stud. Oceanogr.* 56 (15), 918–930. doi:10.1016/j.dsr2.2008.10.034

Tilstone, G. H., Taylor, B. H., Blondeau-Patissier, D., Powell, T., Groom, S. B., Rees, A. P., et al. (2015). Comparison of new and primary production models using SeaWiFS data in contrasting hydrographic zones of the northern north Atlantic. *Remote Sens. Environ.* 156, 473–489. doi:10.1016/j.rse.2014.10.013

Tilstone, G. H., Land, P. E., Pardo, S., Kerimoglu, O., and Van der Zande, D. (2023). Threshold indicators of primary production in the north-east Atlantic for assessing environmental disturbances using 21 years of satellite ocean colour. *Sci. Total Environ.* 854, 158757. doi:10.1016/j.scitotenv.2022.158757

Tiselius, P., Belgrano, A., Andersson, L., and Lindahl, O. (2016). Contribution to the themed section: scaling from individual plankton to marine ecosystems primary productivity in a coastal ecosystem: a trophic perspective on a long-term time series. *J. Plankton Res.* 38 (4), 1092–1102. doi:10.1093/plankt/fbv094

van Leeuwen, S., Tett, P., Mills, D., and van der Molen, J. (2015). Stratified and nonstratified areas in the north sea: long-term variability and biological and policy implications. *J. Geophys. Research-Oceans* 120 (7), 4670–4686. doi:10.1002/2014jc010485

Westberry, T. K., Silsbe, G. M., and Behrenfeld, M. J. (2023). Gross and net primary production in the global ocean: an ocean color remote sensing perspective. *Earth-Science Rev.* 237, 104322. doi:10.1016/j.earscirev.2023.104322

Wilson, R. J., and Heath, M. R. (2019). Increasing turbidity in the north sea during the 20th century due to changing wave climate. *Ocean Sci.* 15 (6), 1615–1625. doi:10.5194/os-15-1615-2019

Wolter, K., and Timlin, M. S. (2011). El nino/southern oscillation behaviour since 1871 as diagnosed in an extended multivariate ENSO index (MEI.ext). *Int. J. Climatol.* 31 (7), 1074–1087. doi:10.1002/joc.2336

Wu, J., Lee, Z.-P., Goes, J., Gomes, H. do R., and Wei, J. (2024). Evaluation of three contrasting models in estimating primary production from ocean color remote sensing using long-term time-series data at oceanic and coastal sites. *Remote Sens. Environ.* 302, 113983. doi:10.1016/j.rse.2023.113983

Xie, Y. Y., Tilstone, G., Widdicombe, C., Woodward, E., Harris, C., and Barnes, M. (2015). Effect of increases in temperature and nutrients on phytoplankton community structure and photosynthesis in the western English Channel. *Mar. Ecol. Prog. Ser.* 519, 61–73. doi:10.3354/meps11101

Zhao, M. S., and Running, S. W. (2010). Drought-induced reduction in global terrestrial net primary production from 2000 through 2009. *Science* 329 (5994), 940–943. doi:10.1126/science.1192666

Zvalinsky, V. I., Lobanova, P. V., Tishchenko, P. Y., and Lobanov, V. B. (2019). Estimation of primary production in the northwestern part of the Sea of Japan by Ship- and satellite-based observations. *Oceanology* 59 (1), 37–48. doi:10.31857/s0030-157459145-55